ESRF	**Experiment title:** *Influence of filament microstructure on the irreversible degradation of high performance Nb3Sn wires under mechanical loads.*	**Experiment number**: MA-2767
Beamline: ID19	**Date of experiment**: from: 30/09/2015 to: 02/10/2015	**Date of report**:
Shifts: 48h/6	**Local contact(s)**: Alexander Rack (alexander.rack@esrf.fr)	*Received at ESRF:*
Names and affiliations of applicants (* indicates experimentalists): Prof. Carmine Senatore (University of Geneva, CH) *, Dr. Christian Barth (CERN, CH) *, Mr. Davide Matera (University of Geneva, CH) *****, Dr. Yuhu Zhai (PPPL, USA) *, Dr. Alexander Rack (ESRF, F) *		

Report:

Published paper: Barth, C. et al. "Quantitative correlation between the void morphology of niobium-tin wires and their irreversible critical current degradation upon mechanical loading". *Sci Rep* 8, 6589 (2018). https://doi.org/10.1038/s41598-018-24966-z

Abstract:

Understanding the critical current performance variation of Nb_3Sn superconducting wires under mechanical loading is a crucial issue for the design of next generation accelerator and fusion magnets. In these applications, the mechanical properties of the conductors may become a limiting factor due to the strong electro-magnetic forces resulting from the combination of large magnets and intense magnetic fields. In particular, the presence of voids in the superconducting filament structure, which are formed during the fabrication and the reaction heat treatment, determines localized stress concentrations and possibly the formation of cracks. In this work, we demonstrate a quantitative correlation between the void morphology and the electro-mechanical limits measured on different Bronze route Nb_3Sn wires. Hot Isostatic Pressing (HIP) prior to the reaction heat treatment is utilized to partially eliminate the voids. The wires' void distributions - with and without HIP treatment - are detected and statistically analyzed using high energy X-ray micro tomography. The stress concentration due to the shape and distribution of the voids as well as their impact on the electro-mechanical properties are determined through finite element method modeling. Finally, the results are quantitatively correlated with the experimentally determined limits of the irreversible critical current degradation upon mechanical loading.

Void detection and analysis:

The X-ray tomography was performed with a photon energy of 89 keV using a 2560 × 2120 pixel resolution detector at beamline ID19. For each acquisition, the sample is rotated 360 °C registering a projection each 0.012° (30'000 projections in total). A spatial sampling of 0.57 µm/pixel was applied.

The post-process analysis of the X-ray tomography data consisted in two consecutive steps. In the first step, the void areas inside the tomography volume were detected from a tomography data set. The detection is done slice by slice using the commercial software package MatLab; each of the slices is cropped and masked to restrict the following void detection and void enhancement steps to the areas containing the sample. Each pixel in the masked area is compared with a threshold which is adjusted to the slice's average brightness and the mean brightness in the region surrounding the pixel to determine if the pixel is a void. This adaptive threshold yields significantly higher detection accuracy than fixed thresholds as variations of the brightness of the images are taken into account [1], see Figure 1-a. The results of these comparisons form a binary 3D matrix which is in the following referred to as the "void matrix". Each entry in the void matrix corresponds to a volume element in the investigated sample of a border length of 0.57 µm. Afterward, a second adaptive threshold is used to distinguish between the filament bundles and the wires' matrix. A three-dimensional binary map of the matrix is assembled. The position of each detected void is correlated with this map to determine if the void is located within a filament bundle, at the interface or within the matrix.

In the second step of the post-processing, the detected void pixels are digitally filtered and grouped into connected void areas which are processed with repeated open and close morphological operations based on Euclidean distance maps. To remove “dark noise”, i.e. isolated pixels in a void region which have not been detected as voids, a distance transformation with a threshold of a few pixels is applied to the void matrix. The 3D view of the voids has been reconstructed, see Figure 1-b, and used as input in mechanical finite elements models.

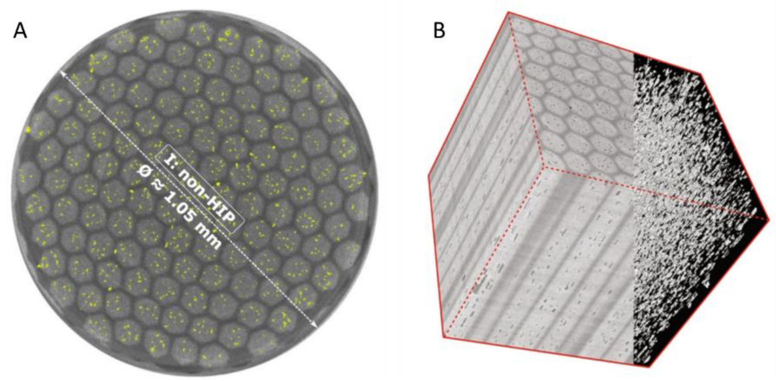

Figure 1 – a) X-Ray tomography of a Nb_3Sn wire, three different elements can be easily identify: copper stabilizer, Nb_3Sn filaments and voids. b) Reconstructed 3D X-ray tomography image of a cube of Bronze Nb_3Sn wire.

***Electro-mechanical measurements*:**

The electro-mechanical properties of all samples were determined using a 4-turn Walters Spring (WASP) system with a total measurement length of 486 mm. The superconductor wire sample was soldered on the outside of a 39 mm diameter titanium-aluminum-vanadium (Ti-6Al-4V) spring [2]. Loading and unloading of the spring changes its diameter straining the sample axially in tension or in compression. The strain was applied in identically spaced steps with a critical current I_c measurement at each step. The strain corresponding to the maximal critical current was obtained by fitting the average critical current vs. strain behaviour of the 4-turns of the WASP. The samples' irreversible strain limit, ε_{irr}, was defined as the first strain from which the backstep results in a 5% lower critical current than the absolute maximal critical current. A “backstep” corresponds to a partial release of strain up to the strain of the maximum critical currentafter a critical current measurement in the tensile region, $I_c(\varepsilon_n)$. In this study ε_{irr} is used as criterion in the comparison with the numerical FEM simulations

Mechanical finite element method model:

After the image post process, the size and the relative position of the connected void areas were analysed by an approximation with ellipsoids. Such an approximation strongly increases the regularity by reducing the shape complexity of the voids, a necessary step to obtain void data adequate for FEM model input.

To determine the effect of the voids as stress concentrators, a 0.1 mm thick disk of the wire was modelled with the finite element method in real dimensions using the solid mechanics component of the commercial software package COMSOL Multiphysics. Internal features of the wire are implemented down to the filament bundles, a resolution similar to what is achieved which the X-ray tomography. The voids are added to the model as ellipsoids in iterative algorithms with distances, sizes, shapes and orientation taken from the histograms of the X-ray tomography analysis. One side of the wire is fixed while a displacement is imposed as a boundary condition on the other to apply a mechanical strain. In the FEM simulations, the strain is applied to the wires, as determined from the electro-mechanical measurement, through a displacement boundary condition to determine the critical stress value.

The baselines were modelled 12 times, each run with a unique distribution of the voids, and the von Mises stress distribution within the Nb_3Sn bundles was determined. 12 separate runs of the model are deemed sufficient to cope with the variations of the statistical void distribution in order to gain sound averaged values. Over the 12 runs, the model defines an irreversible strain limit, ε_{irr}, ranging between 0.490% and 0.511% with an average of 0.50%, in agreement with the 0.48% from the experimental results.

Conclusion:

A correlation between the voids and the electro-mechanical properties was validated for Bronze route Nb_3Sn wires using FEM models. Thanks to the void morphology obtained from the X-ray tomography as input, it was possible to clarify that not only the total void fraction in the wire but also the shapes of voids play a major role. The FEM results are in very good agreement with the electro-mechanical axial WASP measurements.

***References*:**

[1] D. Bradley, G. Roth, Journal of Graphics Tools, 12 (2007) 13-21.

[2] D. Uglietti, B. Seeber, V. Abächerli, A. Pollini, D. Eckert, R. Flükiger, Superconductor Science and Technology, 16 (2003) 1000-1004.